Diagnostic Pathology: Open Access
ISSN: 2476-2024
Oh et al, Diagn Pathol Open 2022, S12:003
Research Article Open Access

Keloid-specific Gene Expression Profiling for Accurate Diagnostic and Therapeutic Applications

Yoojeong Oh[4], Jaemyun Lyu[2,7], Karthika Muthuramalingam[2], Eunmyong Lee[3], Miae Choi[1], Insuk Sohn[2], Jong-Hee Lee[5] and Seok-Hyung Kim[1,4,6*]

[1]*Department of Pathology, Sungkyunkwan University School of Medicine, Seoul, Republic of Korea*
[2]*Arontier Inc., Seoul, Republic of Korea*
[3]*InnoCure Therapeutics Inc., Seoul, Republic of Korea*
[4]*Department of Health Science and Technology, Sungkyunkwan University, Seoul, Republic of Korea*
[5]*Department of Dermatology, Sungkyunkwan University School of Medicine, Seoul, Republic of Korea*
[6]*Single Cell Network Research Center, Suwon, Republic of Korea*
[7]*RNA Cell Biology Lab, Seoul, Republic of Korea*

Abstract

Scars are a heterogeneous disease including normotrophic scars, hypertrophic scars, and keloids. Of these lesions, keloids are a distinct subtype from any other type of scar. Clinically, it causes pain, itching, or tenderness, causing life discomfort and characteristically irreversible.

Despite various treatment modalities, restoring keloids to normal tissues is difficult, and frequent recurrences have been reported. Therefore, it is essential to identify keloid-specific genes for accurate diagnosis and treatment of keloids. In an effort to find out keloid-specific genes, several studies compared keloids with scar-free normal skin, which leading general scar-related genes to be chosen rather than keloid-specific genes. To select for highly accurate keloid-specific genes and pathways, we compared the transcriptome profile of keloids with those of normotrophic scars and hypertrophic scars, which acquired from formalin-fixed paraffin-embedded human skin samples using high-throughput RNA-sequencing techniques. Differential expression analyses and over-representation analyses revealed that genes related to nervous system process were upregulated in keloids, whereas genes related with immune responses were downregulated in keloids. Additionally, the extracellular matrix related processes were highlighted in both hypertrophic scars and keloids. Finally, we highlight potential keloid-specific biomarkers and expression changes that can be employed for future therapeutics of keloids.

Keywords: Normotrophic scar; Hypertrophic scar; Keloid; RNA sequencing; Scar management

Introduction

A scar is an area of fibrous tissue that replaces normal skin after an injury. Scarring is a biological process of wound healing. Despite tremendous progress in unravelling the science behind wound healing, the mechanisms for elucidating scar formation caused by abnormal wound healing are still unknown [1]. Deep injury to the reticular dermis sometimes results in pathological abnormal fibrous scars such as hypertrophic scars and keloids, which are thought to be caused by abnormal wound healing due to altered gene expression in the wound healing tissue. Hypertrophic scars and keloids consist of numerous inflammatory cells, proliferating fibroblasts, progressive collagen deposition and enhanced angiogenesis [2-4]. And they present distinct clinical, histological, and developmental features. Clinically, hypertrophic scars are confined within the wound boundary, while keloids extend growth beyond the wound borders [5,6]. Histologically, hypertrophic scars have fewer thick collagen fibers than keloids [7,8]. Furthermore, hypertrophic scar tissues are composed of low-density Dermatan Sulfate (DS) proteoglycans, while keloid scar tissues are composed of both low-density DS and Chondroitin Sulfate (CS) proteoglycans, with CS proteoglycans in higher proportion [9,10]. Hypertrophic scars usually develop within two months from injury and tend to regress over time. In contrast, keloids develop and progress after 3 months or more, grow irreversibly for years, and cause medical problems as well as life problems such as itchiness and unusual appearance for patients [11]. Hypertrophic scars tend to respond well to treatment. On the other hand, once formed, keloids are very difficult to restore to normal tissues, and frequent recurrences and exacerbations over a long period of time become another obstacle to treatment [12]. It has not been reported yet what kind of scars would be occurred when the skin is damaged. Therefore, it is essential to understand the pathological factors behind the various scar types and gene expression profiles of pathological scars caused by abnormal wound healing, for the development of efficient treatment strategies for the treatment of abnormal scars.

To date, there have been five reports comparing gene expression patterns in keloid and related scar lesions using whole transcriptome analysis such as cDNA microarray or RNA-seq. Onoufriadis, et al. and Wu, et al. performed RNA-seq on keloids and normal skin tissue [13,14]. Hahn, et al. Chao-Kai, et al. and Matsumoto, et al. compared mRNA expression patterns between keloids and normal skin tissue using cDNA microarrays [15-17]. Although these studies have provided new

***Corresponding author:** Dr. Seok-Hyung Kim, Department of Health Science and Technology, Sungkyunkwan University, Seoul, Republic of Korea, E-mail: platoshkim@gmail.com

Received: 20-Oct-2022, Manuscript No. DPO-22-77863; **Editor assigned:** 21-Oct-2022, PreQC No. DPO-22-77863(PQ); **Reviewed:** 04-Nov-2022, QC No DPO-22-77863; **Revised:** 14-Nov-2022, Manuscript No. DPO-22-77863(R); **Published:** 21-Nov-2022, DOI: 10.4172/ 2476-2024.7.S12.003

Citation: Oh Y, Lyu J, Muthuramalingam K, Lee E, Choi M, et al. (2022) Keloid-specific Gene Expression Profiling for Accurate Diagnostic and Therapeutic Applications. Diagnos Pathol Open 7:003.

insights into keloids, there are limitations in that the selected keloid-specific gene expression profile could not be distinguished from a scar-related genes expression profile, since they compared keloids to scar-free normal skin tissue not to reversible scars. Considering different responses of irreversible keloids and reversible hypertrophic scars to the treatment, it is crucial to compare the overall gene expression patterns of irreversible scars such as keloids and reversible scars. In this study, we aimed to compare the overall gene expression patterns of reversible and irreversible scars and provide insight into the molecular and cellular mechanisms behind these lesions. Toward this goal, high-throughput RNA-sequencing techniques using next-generation sequencing technology were employed. By elucidating highly specific genes and related signaling pathways for abnormal fibroproliferative scar lesions, this study can contribute to the development of effective and targeted therapeutic strategies for these lesions.

Materials and Methods

Patients and tissue samples

Tissue samples were obtained from the biobanks at the Samsung medical center, Seoul, Republic of Korea. All patients provided informed consent and the study was performed according to internal ethics review board approvals at Samsung medical center. Four keloid tissue samples, five hypertrophic scars tissue samples and three mature scar tissue samples were obtained after a thorough histopathological examination and clinical manifestations of patients. All experiments involving humans were performed in adherence to the Helsinki Guidelines. These samples were fixed in formalin, embedded in paraffin, and stained with hematoxylin and eosin.

RNA isolation

Consecutive 10 μm sections were generated from each of the FFPE cell blocks using a standard microtome blade. Deparaffinization of FFPE samples was performed using xylene at room temperature for 30 min followed by two washes with 100% ethanol. Then lesion of each slide was manually dissected. The manual isolation of RNA was performed using RNeasy Mini Kit (Qiagen GmbH, Hilden, Germany) according to manufacturers' instructions. RNA concentration was measured using the NanoDrop 1000 spectrophotometer (Thermo Fisher Scientific) and RNA quality was evaluated with RNA 6000 Pico LabChip kit by using BioAnalyzer 2100 microcapillary electrophoresis system (Agilent Technologies, Inc., Santa Clara, CA USA). Reverse transcription was performed using Transcriptor First Strand cDNA Synthesis Kit (Roche Applied Science) from 250 ng of total RNA and the combination of anchored-oligo(dT) and random hexamer primers.

Next-generation sequencing

For library preparation, the Illumina TruSeq RNA Access Library Prep Kit (Cat. No. 20020189, Illumina, San Diego, CA, USA) was used with 40 ng of FFPE RNA. The libraries were prepared according to the manufacturer's protocol with the following change for the FFPE samples: the hybridization/capture was performed individually instead of as pooled samples after the first PCR step. Library concentrations were adjusted to 1 nM and pooled for multiplex sequencing. Pooled libraries were denatured and diluted to 7.5 pM and were sequenced on the Illumina HiSeq 2500 Platform to 101bp paired-end reads.

Data processing and quantification

Adaptor sequences were trimmed out with Cutadapt (version 2.3) and read shorter than 50 base pair after trimming were filtered out [18]. All reads were aligned to the human reference genome and corresponding gene annotation (Gencode V22) with STAR aligner 2-pass mode (version 2.4.2a) [19]. Aligned reads were quantified in gene level, by HTSeq (version 0.12.4) with "intersection-nonempty" mode [20]. Multidimensional scaling analysis were processed via clustermap function of python seaborn package (version 0.11.1) with log2 (FPKM+1) values using genes with mean FPKM>1 among the samples. tSNE plots were visualized with Rtsne packages [21].

Differential expression with ensemble approaches

We implemented an ensemble approach for differential gene expression analysis. From all quantified counts of HTSeq, we performed 3 independent differential gene expression analysis with the most commonly used methods, Limma-voom, edgeR, and DESeq2, for Hypertrophic Scar vs. Scar and Keloid vs. Hypertrophic Scar comparisons [22-24]. We discarded low read count genes below 3 for all samples within tissue types. We applied cut-off on limma-voom and DEseq2, log2 fold change>1 and adjusted P-Value<0.1, and on edgeR, abs (log2 fold change)>1 AND FDR<0.1, for enlisting differentially expressed genes. After getting 3 differentially expressed gene lists of Hypertrophic Scar vs. Scar, we overlapped 3 lists and genes with 2 or more than 2 methods regarded as differentially expressed genes for ensemble approaches.

Over-representation analysis

Over-representation analyses were performed with Enrichr via GSEAPY (version 0.9.19) user predefined GO_Biological_Process_2015 and KEGG_Human_2019 gene sets enrichment analyses. Adjusted P-value<0.1 was applied [25].

Public high-throughput normal data collection and processing

For comparison over Keloid and normal tissue, we downloaded raw sequenced reads from GEO via accession number GSE113619. Among sequenced samples, Day 0 of the normal cases (13 samples) was regarded as normal tissue samples. Analysis over Keloid vs. Normal tissue was processed with the same ensemble approaches implemented. Since Keloid and normal tissue comparison have more biases because of using two different experimental procedures, we applied higher cutoff as log2 fold change >3 and adjusted P-Value<0.0001 on DEGs. Over-representation analyses were processed in the same methods as previously described.

Results

Expression analysis of keloids and related lesions through RNA-seq

WTo reveal the gene expression characteristics of keloids and related lesions, we collected 4 keloid tissues, 5 hypertrophic scars, and 3 normotrophic scars. The three types of lesions were categorized by characteristic appearance, histological morphology and clinical features [26]. From normotrophic scars and hypertrophic scars to keloids, the epidermal cell layer becomes thicker and the collagen fibers become thicker and denser. Consistent with previous reports, keloids and hypertrophic scars showed abundant vasculature, high mesenchymal cell density, inflammatory cell infiltration, and thickened epidermal cell layer compared to normotrophic scars [27,28]. In particular, thick collagen fibers composed of numerous tightly packed fibrils were observed in keloids, while hypertrophic scars exhibit a nodular structure composed of fibroblasts, small blood vessels, and randomly

organized collagen fibers [29].

To confirm the histopathologic classification of the samples, the expression profiles of these collected tissue samples were analyzed by unsupervised clustering using a machine learning-based dimensionality reduction algorithm such as MDS (Multi-Dimensional Scaling) and tSNE (t-Distributed Stochastic Neighbor Embedding). The results showed that these lesions were separated into three clusters, relatively consistent with their diagnoses. The differential genes of these normotrophic Scar (S), Hypertrophic Scar (HS), and Keloid (K) were grouped into 8 classes depending on expression pattern: ○1 UU (Up-Up, S<HS<K), ○2 UF (Up-Flat, S<HS~K), ○3 FD (Flat-Down, S~HS>K), ○4 UD (Up-Down, S<HS>K), ○5 DD (Down-Down, S>HS>K), ○6 DF (Down-Flat, S>HS~K), ○7 FU (Flat-Up, S~HS<K), and ○8 DU (Down-Up, S>HS<K). The genes were separated as upregulated (U), downregulated (D), or not differentially expressed (F). Expression pattern of grouped genes over scar types were also separated in patterns as expected (Figure 1) (Table 1).

Type of tissue	Gender and Age	Body part effected
Normotrophic Scar #1	F 56	Skin, Scalp
Normotrophic Scar #2	F 57	Skin, back
Normotrophic Scar #3	F 35	Skin, public area
Hypertropic Scar #1	F 55	Skin, neck
Hypertropic Scar #2	M 69	Skin, right thigh
Hypertropic Scar #3	M 68	Skin, post-auricular area
Hypertropic Scar #4	F 81	Skin, right breast
Hypertropic Scar #5	M 66	Skin, left cheek
Keloid #1	F 21	Skin, ear
Keloid #2	F 19	Skin, ear
Keloid #3	F 53	Skin, abdomen
Keloid #4	M 15	Skin, ear
Note: (■) Normotrophic Scar; (■) Hypertropic Scar; (■) Keloid		

Table 1: Summary of information on scar tissues used in this study.

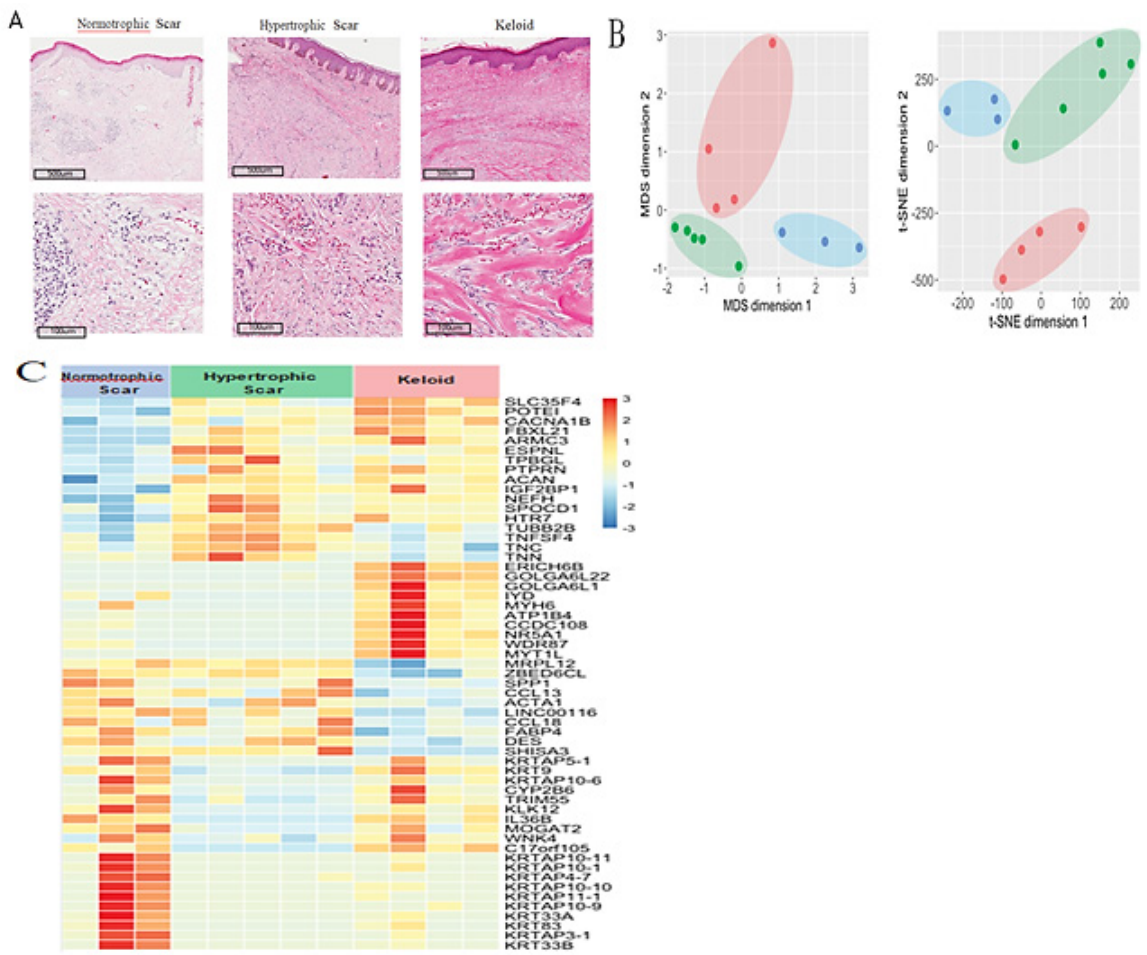

Figure 1: Differences in the pathology and gene expression patterns of normotrophic scars, hypertrophic scars, and keloids. A. From normotrophic scars and hypertrophic scars to keloids, the epidermal cell layer becomes thicker and the collagen fibers become thicker and denser; B. MDS and tSNE clustering of 12 skin tissues. Tissues are color coded by an algorithm for determining expression clusters and tissue types; C. Heat map of gene expression grouped under different expression models across the three types of scars.

Derivation of keloid-specific genes and signaling pathways by comparing gene expression profiles of keloids and reversible scars

Once keloids were developed, they grow irreversibly for years, compared to normoptophic and hypertrophic scars which regress over time. In an attempt to discover genes specifically regulated in keloids as irreversible scars, we classified normotrophic and hypertrophic scars as one group-reversible scar and compared their gene expression profiles with that of keloids. To identify genes specifically up or downregulated in keloids, we performed mRNA sequencing and differential expression analysis on RNA-Seq data from normotrophic scars, hypertrophic scars, and keloids with following statistical methods. For differential expression analysis, we implemented Ensemble approaches as three widely used methods (Limma-voom, edgeR and DESeq2) to achieve lower false positive DEGs. In this approach, genes were flagged as DEG on at least two different analyses was used for further analysis. Overall, 195 genes were downregulated in keloids compared with reversible scars, whereas 306 genes were upregulated in keloids. Of these genes, golgin A6 family genes and *ERICH6B* (Glutamate-Rich 6B) genes were identified as the most significantly changed genes as described in volcano plots. It should be noted that the levels of golgin A6 family genes and *ERICH6B* genes were not only significantly changed, but also exhibited the highest magnitude of fold change among the genes in keloids compared with reversible scars. Golgins are a family of predominantly coiled-coil proteins that are localized to the Golgi apparatus [30]. Anchored to the Golgi membrane, they are predicted to project into the surrounding cytoplasm and are involved in various functions of the Golgi apparatus, such as vesicular traffic through golgin-mediated tethering. Second, golgins are involved in maintenance and positioning of the Golgi apparatus within cells. In addition to acting as tethers, some golgins can sequester various factors at the Golgi membrane, allowing spatiotemporal regulation of downstream cellular functions. However, the specific functions and clinical relevance of the Golgin A6 family has not been elucidated yet. In the case of *ERICH6B*, there is little information on the structure, function and clinical relevance of the gene, except for its predominant expression in the testis.

Next, up and downregulated 501 DEGs (up: 306, down: 195) was classified as expression changes on normotrophic scars-hypertrophic scars-keloids. Specifically, most of the downregulated DEGs in keloids belonged to the FD (Flat-Down, 64.6%) subgroup, in contrast to very few belonged to DD (Down-Down, 0%) or DF (Down-Flat, 5.6%) subgroup. On the other hand, most of upregulated DEGs in keloids belonged to the FU (Flat-Up, 67.3%) subgroup, while very few belonged to UU (Up-Up, 1.0%) or UF (Up-Flat, 1.0%) subgroup. These results indicate that most of the DEGs exhibited small differences between normotrophic and hypertrophic scars but were higher or lower in keloids.

For better understanding of biological function of genes that exhibited specifically high or low expression in keloids. DEGs are enriched to Gene Ontology (GO) and Kyoto Encyclopedia of Genes and Genomes (KEGG) pathway. Over-representation analysis on GO Biological Process showed that the genes involved in 'activation of immune response', 'antigen processing and presentation of peptide antigen' and 'immunoglobulin mediated immune response' are significantly downregulated in keloids. These findings suggest that immune regulation and inflammatory mechanisms play important roles in keloid formation. On the other hand, DEGs upregulated in keloids were over-represented in roles of 'sensory perception', 'neuron development', and 'muscle filament sliding'. Over-representation analysis on KEGG pathway demonstrated that downregulated DEGs in keloids were enriched in 'systemic lupus erythematosus' and 'antigen processing and presentation', whereas upregulated DEGs in keloids were enriched in 'protein digestion and absorption' and 'insulin secretion'. Overall, downregulated DEGs in keloids were associated with immune functions, whereas upregulated DEGs in keloids were associated with neuron development and muscle contraction. In keloids, the regulation of T cell proliferation and negative regulation of T cell activation were specifically downregulated, whereas visual/sensory perception was specifically upregulated. In addition, the systemic lupus erythematosus pathway was downregulated, whereas the pathways of protein digestion and absorption were upregulated. (Figure 2) (Tables 2-5).

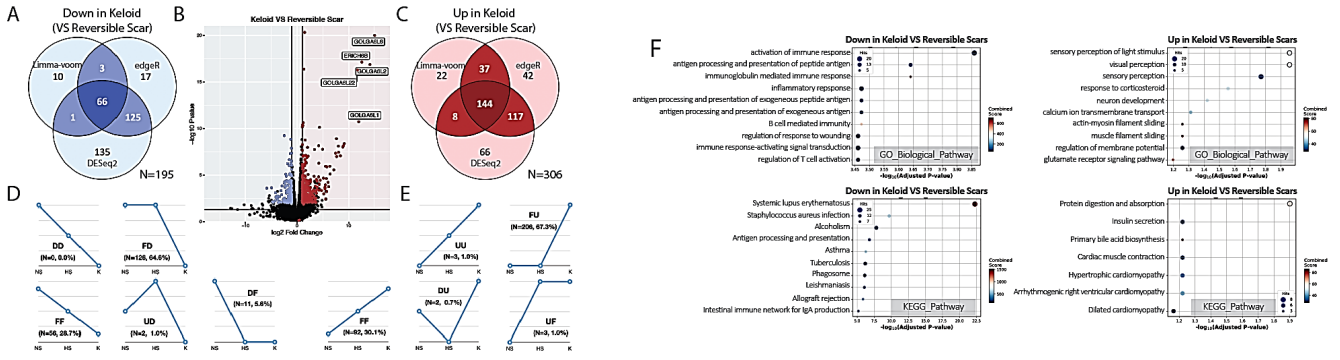

Figure 2: Differentially expressed genes (DEGs) specifically upregulated and downregulated in keloids compared to normotrophic scars and hypertrophic scars. A and C. Venn diagrams represent the intersection of DEGs between keloid and reversible scars derived by three different methods (Limma-voom, DESeq2 and edgeR). Compared with keloid and reversible scars, downregulated DEGs were a total of 195, and upregulated DEGs were a total of 306; B. Volcano plot of DEGs showing the standardized mean difference and the adjusted p-value for the 501 genes; D. Downregulated DEGs in keloids compared to reversible scars can be divided into five patterns: DD (Down-Down), FD (Flat-Down), DF (Down-Flat), UD (Up-Down), FF (Flat-Flat); E. The five patterns of up-regulated DEG can be classified as follows: UU (Up-Up), FU (Flat-Up), UF (Up-Flat), DU (Down-Up), FF (Flat-Flat); F. Results of GO enrichment analysis and KEGG pathway classification enrichment analysis for keloids specific DEGs.

GO ID	Term	Overlap	Adjusted P-value	Genes
GO:0002253	Activation of immune response	20/487	0.000138	*CD86, HLA-DRB5, FCER1G, CTSS, PYCARD, FCGR3A, FCGR2A, C3AR1, HLA-DPB1, CDK1, TLR8, HLA-DRA, CD36, VSIG4, PIK3AP1, FCGR1A, HLA-DRB1, CTSB, C1QC, HLA-DPA1*
GO:0048002	Antigen processing and presentation of peptide antigen	12/185	0.000228	*BCAP31, CD74, HLA-DRB5, FCER1G, HLA-DPB1, HLA-DRA, CD36, FCGR1A, HLA-DRB1, CTSS, PSMA7, HLA-DPA1*
GO:0016064	Immunoglobulin mediated immune response	5/16	0.000228	*CD74, FCER1G, TLR8, FCGR1A, HLA-DRB1*
GO:0006954	Inflammatory response	16/376	0.000337	*IL10, CCL13, CD163, SERPINA1, TNFAIP6, LY86, LYZ, AIF1, PYCARD, C3AR1, SPP1, BDKRB2, TLR8, CCL18, FCGR1A, HLA-DRB1*
GO:0002478	Antigen processing and presentation of exogenous peptide antigen	11/171	0.000337	*CD74, HLA-DRB5, FCER1G, HLA-DPB1, HLA-DRA, CD36, FCGR1A, HLA-DRB1, CTSS, PSMA7, HLA-DPA1*
GO:0019884	Antigen processing and presentation of exogenous antigen	11/173	0.000337	*CD74, HLA-DRB5, FCER1G, HLA-DPB1, HLA-DRA, CD36, FCGR1A, HLA-DRB1, CTSS, PSMA7, HLA-DPA1*
GO:0019724	B-cell mediated immunity	5/20	0.000337	*CD74, FCER1G, TLR8, FCGR1A, HLA-DRB1*
GO:1903034	Regulation of response to wounding	15/347	0.000346	*IL10, FCER1G, SCARA5, CMA1, CAV1, PLA2G7, F3, CTSS, FABP4, ALOX5AP, SPP1, CD36, PIK3AP1, FCGR1A, HLA-DRB1*
GO:0002757	Immune response-activating signal transduction	17/440	0.000346	*CD86, HLA-DRB5, FCER1G, CTSS, FCGR3A, FCGR2A, C3AR1, HLA-DPB1, CDK1, TLR8, HLA-DRA, CD36, PIK3AP1, FCGR1A, HLA-DRB1, CTSB, HLA-DPA1*
GO:0050863	Regulation of T cell activation	13/259	0.000346	*IL10, CD86, CD74, HLA-DRB5, CAV1, AIF1, PYCARD, HLA-DPB1, HLA-DRA, VSIG4, IL7R, HLA-DRB1, HLA-DPA1*

Table 2: GO Biological Process enrichment result for down regulated DEGs in Keloid VS. Reversible Scars.

Term	Overlap	Adjusted P-value	Genes
Systemic lupus erythematosus	25/133	3.21E-25	*CD86, HIST1H2BM, HIST1H2BO, FCGR3A, HIST1H3A, HIST1H3H, HIST1H3B, FCGR1A, HIST1H2AB, HLA-DPA1, HIST1H2AM, IL10, HLA-DRB5, HIST1H4L, HIST1H2AJ, HIST1H4A, HIST1H4B, FCGR2A, HIST4H4, HLA-DPB1, HLA-DRA, HIST1H2BH, HIST1H4C, HLA-DRB1, C1QC*
Staphylococcus aureus infection	12/68	2.37E-12	*IL10, FCGR3A, HLA-DRB5, FCGR2A, C3AR1, HLA-DPB1, HLA-DRA, FPR3, FCGR1A, HLA-DRB1, HLA-DPA1, C1QC*
Alcoholism	15/180	2.76E-10	*HIST1H2AM, HIST1H2BM, HIST1H2BO, MAOB, HIST1H4L, HIST1H2AJ, HIST1H4A, HIST1H3A, HIST1H4B, HIST4H4, HIST1H2BH, HIST1H3H, HIST1H3B, HIST1H4C, HIST1H2AB*
Antigen processing and presentation	10/77	3.83E-09	*CD74, HLA-DRB5, HLA-DPB1, HLA-DRA, HSPA2, CTSS, HSPA1B, HLA-DRB1, CTSB, HLA-DPA1*
Asthma	7/31	1.62E-08	*IL10, HLA-DRB5, FCER1G, HLA-DPB1, HLA-DRA, HLA-DRB1, HLA-DPA1*
Tuberculosis	13/179	2.33E-08	*IL10, CD74, HLA-DRB5, FCER1G, CTSS, FCGR3A, FCGR2A, HLA-DPB1, HLA-DRA, FCGR1A, ATP6V0C, HLA-DRB1, HLA-DPA1*
Phagosome	12/152	3.25E-08	*MSR1, HLA-DRB5, FCGR3A, FCGR2A, HLA-DPB1, HLA-DRA, CD36, FCGR1A, ATP6V0C, HLA-DRB1, CTSS, HLA-DPA1*
Leishmaniasis	9/74	4.23E-08	*IL10, FCGR3A, HLA-DRB5, FCGR2A, HLA-DPB1, HLA-DRA, FCGR1A, HLA-DRB1, HLA-DPA1*
Allograft rejection	7/38	7.35E-08	*CD86, IL10, HLA-DRB5, HLA-DPB1, HLA-DRA, HLA-DRB1, HLA-DPA1*
Intestinal immune network for IgA production	7/48	3.95E-07	*CD86, IL10, HLA-DRB5, HLA-DPB1, HLA-DRA, HLA-DRB1, HLA-DPA1*

Table 3: KEGG Pathway enrichment result for down regulated DEGs in Keloid VS. Reversible Scars.

GO ID	Term	Overlap	Adjusted P-value	Genes
GO:0050953	sensory perception of light stimulus	13/198	0.0111	*TULP1, RPGR, COL1A1, RP1L1, OCLM, RIMS1, CACNB2, RP1, GRM8, SIX3, CNGB3, PPEF2, GPR179*
GO:0007601	visual perception	13/195	0.0111	*TULP1, RPGR, COL1A1, RP1L1, OCLM, RIMS1, CACNB2, RP1, GRM8, SIX3, CNGB3, PPEF2, GPR179*
GO:0007600	sensory perception	20/457	0.017	*TAS2R60, EYA1, COL11A2, CACNA1D, TULP1, SLC6A3, RPGR, COL1A1, RP1L1, OCLM, CACNB2, RIMS1, RP1, MYO15A, GRM8, SIX3, CNGB3, ASIC3, PPEF2, GPR179*
GO:0031960	response to corticosteroid	10/140	0.0278	*COL1A1, MSTN, UCN2, WNT7B, BCKDHB, PDX1, GRIK4, FOSB, FOS, SOX30*
GO:0048666	neuron development	9/121	0.038	*ALK, ROBO2, TMC1, RP1L1, RP1, TULP1, HOXD10, GLI2, RPGR*
GO:0070588	calcium ion transmembrane transport	9/128	0.0487	*TMC1, CACNB2, RYR2, CACNG8, IL1RAPL1, CACNA1B, CACNA1D, ATP2A1, TRPM4*
GO:0033275	actin-myosin filament sliding	5/38	0.0551	*MYH2, ACTN2, MYH8, MYH4, MYH7*
GO:0030049	muscle filament sliding	5/38	0.0551	*MYH2, ACTN2, MYH8, MYH4, MYH7*
GO:0042391	regulation of membrane potential	13/266	0.0551	*RYR2, KCNE2, ACTN2, CACNA1B, CACNA1D, GRIK2, RIMS1, NETO1, GJA5, CHRNE, CNGB3, TRPM4, SHANK1*
GO:0007215	glutamate receptor signaling pathway	5/40	0.0634	*GRM5, GRM8, GRIK4, GRIK2, CDK5R1*

Table 4: GO Biological Process enrichment result for up regulated DEGs in Keloid VS. Reversible Scars.

Term	Overlap	Adjusted P-value	Genes
Protein digestion and absorption	8/90	0.0125	*COL1A1, COL27A1, MEP1B, COL22A1, COL7A1, COL11A2, ATP1B4, SLC16A10*
Insulin secretion	6/86	0.0601	*RYR2, CCKAR, PDX1, ATP1B4, CACNA1D, TRPM4*
Primary bile acid biosynthesis	3/17	0.0601	*CYP46A1, BAAT, CYP7A1*
Cardiac muscle contraction	6/78	0.0601	*RYR2, CACNB2, CACNG8, ATP1B4, CACNA1D, MYH7*
Hypertrophic Cardiomyopathy (HCM)	6/85	0.0601	*RYR2, CACNB2, CACNG8, ITGA2B, CACNA1D, MYH7*
Arrhythmogenic Right Ventricular Cardiomyopathy (ARVC)	6/72	0.0601	*RYR2, CACNB2, CACNG8, ACTN2, ITGA2B, CACNA1D*
Dilated Cardiomyopathy (DCM)	6/91	0.0685	*RYR2, CACNB2, CACNG8, ITGA2B, CACNA1D, MYH7*
Glutamatergic synapse	6/114	0.166	*GRM5, GRM8, GRIK4, CACNA1D, GRIK2, SHANK1*
Calcium signaling pathway	8/188	0.166	*RYR2, GRM5, CCKAR, PLCZ1, CACNA1B, CACNA1D, ATP2A1, MYLK3*
Taurine and hypotaurine metabolism	11/02	0.2	*GADL1, BAAT*

Table 5: KEGG Pathway enrichment result for up regulated DEGs in Keloid VS. Reversible Scar.

Keloids and hypertrophic specific upregulated DEGs are predominantly associated with remodeling of extracellular matrix structural tissue

Hypertrophic scars and keloids have a commonality in that they are present in abnormally high levels in fibroproliferative lesions. To gain insight into the mechanisms behind this abnormality, we attempted to identify DEGs that are specifically upregulated in hypertrophic scars and keloids. Our study revealed 88 upregulated genes in these exaggerated scars compared to normotrophic scars, including RYR2 (ryanodine receptor 2), ARMC3 (armadillo repeat including 3), and SMCO2 (single-pass membrane protein with coiled-coil domains 2) as representative genes with larger fold changes. Particularly, these 88 DEGs were highly over-represented on 'extracellular structure/matrix organization' among GO Biological Process terms. Overall, these results are in consistently implies that the clinical observation of excessive ECM depositions are represented in both hypertrophic scars and keloids (Tables 6 and 7).

Keloids and hypertrophic scar specific downregulated DEGs are associated with keratinization, epidermal development, and the estrogen signaling pathway

Compared to upregulated genes, we identified 809 downregulated genes in exaggerated scars such as hypertrophic scars and keloids. Over representation analysis on GO Biological Process terms found most represented terms as 'keratinization' and 'epidermal development'. Also, in KEGG pathways, 'estrogen signaling pathway' was the most represented term (Figure 3) (Tables 8 and 9).

Hypertrophic scar specific genes are associated with epidermal cell differentiation and the lipid catabolic process

Although hypertrophic scars are reversible, the degree of fibrosis is more severe and prolonged compared to that of normotrophic scars. Therefore, we attempted to find hypertrophic scar-specific genes to distinguish them from both keloids and normotrophic scars. Only four DEGs specifically were upregulated in hypertrophic scars, including TUBB2B (tubulin, beta 2B class 2 B), TNFSF4 (tumor necrosis factor superfamily, member 4), TNC (tenascin C), and TNN (tenascin N). In contrast, a total of 237 DEGs was specifically downregulated in hypertrophic scars. Among the mostly changed genes in fold changes, KRTAP5-1 (keratin associated protein 5-1), KRT9 (keratin9), and KRTAP10-6 (keratin associated protein 10-6) are commonly related to keratin. Over-representation analysis results on GO Biological processes revealed that these hypertrophic scar specific expressions were associated with 'epidermal cell differentiation', 'epidermal development', and 'water homeostasis. Conversely, over-represented KEGG pathway terms were 'arachidonic acid metabolism', 'linoleic acid metabolism' (Figure 4) (Tables 10 and 11).

Scar-free normal skin is not a proper control group for determining keloid-specific genes

Previous studies have used scar-free normal skin as a control for comparison with keloids. Since keloids are a possible outcome of wound healing, it is uncertain if it is appropriate to compare keloids with unwounded skin tissue. This limitation suggests that documented studies comparing keloids with scar-free normal skin as a control group are including expression profiles of overall scars rather than keloid-specific characteristics. To overcome this issue, we hypothesized that comparing expression profiles between types of scar tissues would find scar subtype specific features better than comparison between keloid and scar-free normal tissue. For scar-free normal comparisons, we imported publicly available normal skin tissue data from GEO (ID: GSE113619). We implemted the same Ensemble approaches on differential expression analysis and identified DEGs. According to over representation analyses with those DEGs, expression profile changes of keloids, hypertrophic scars, and normotrophic scars than normal skin present very similar shared results especially in GO Biological Processes. Specifically, the genes for 'extracellular matrix/structure organization' and 'extracellular matrix assembly' were upregulated in all three types of scars compared to normal skin. In addition, the genes for 'keratinization', 'epidermal development', and 'epithelial cell differentiation' were downregulated in all three types of scars. These results imply previous studies that directly compared keloids with scar-free normal skin were more likely to discover general scar-specific features rather than keloid-specific features. Therefore, keloid-specific features can be found better by comparing keloids with other reversible scars instead of with scar free normal skin. From these scar tissue type based comparisons, the keloid-specific genes obtained from this improved comparison were related to sensory perception, neuron development, activation of the immune response, and the lipid biosynthetic process (Figure 5) (Tables 12-17).

GO ID	Term	Overlap	Adjusted P-value	Genes
GO:0043062	Extracellular structure organization	15/360	2.97E-08	*ITGB1, POSTN, OLFML2B, TGFB3, PLOD2, NID2, GDF5, ADAMTS4, ACAN, MMP14, ADAMTS14, BMP1, ITGA10, SH3PXD2B, EMILIN1*
GO:0030198	Extracellular matrix organization	15/359	2.97E-08	*ITGB1, POSTN, OLFML2B, TGFB3, PLOD2, NID2, GDF5, ADAMTS4, ACAN, MMP14, ADAMTS14, BMP1, ITGA10, SH3PXD2B, EMILIN1*
GO:0010975	Regulation of neuron projection development	9/275	0.00139	*PTPRD, NTRK1, ITGB1, FRMD7, MAP1B, NCS1, NEFL, FAT3, EPHA3*
GO:0001501	Skeletal system development	7/162	0.00206	*ADAMTS4, ACAN, POSTN, BMP1, SH3PXD2B, ALPL, PAPSS2*
GO:0031344	Regulation of cell projection organization	10/391	0.00206	*PTPRD, NTRK1, ITGB1, FRMD7, TGFB3, MAP1B, NCS1, NEFL, FAT3, EPHA3*
GO:0045664	Regulation of neuron differentiation	10/405	0.00233	*PTPRD, NTRK1, ITGB1, FRMD7, MAP1B, NCS1, NEFL, FAT3, GDF5, EPHA3*
GO:0031346	Positive regulation of cell projection organization	7/195	0.00427	*PTPRD, NTRK1, ITGB1, TGFB3, MAP1B, NEFL, EPHA3*
GO:0010720	Positive regulation of cell development	9/358	0.00428	*PTPRD, NTRK1, ITGB1, TGFB3, MAP1B, SNAI1, NEFL, GDF5, EPHA3*
GO:0010976	Positive regulation of neuron projection development	6/144	0.00562	*PTPRD, NTRK1, ITGB1, MAP1B, NEFL, EPHA3*
GO:0045666	Positive regulation of neuron differentiation	7/217	0.00562	*PTPRD, NTRK1, ITGB1, MAP1B, NEFL, GDF5, EPHA3*

Table 6: GO Biological Process enrichment result for UF pattern of DEGs.

Term	Overlap	Adjusted P-value	Genes
Hypertrophic Cardiomyopathy (HCM)	4/85	0.0363	*ITGB1, RYR2, TGFB3, ITGA10*
Dilated Cardiomyopathy (DCM)	4/91	0.0363	*ITGB1, RYR2, TGFB3, ITGA10*
Arrhythmogenic Right Ventricular Cardiomyopathy (ARVC)	3/72	0.137	*ITGB1, RYR2, ITGA10*
Amyotrophic Lateral Sclerosis (ALS)	2/51	0.476	*NEFL, NEFH*
Pathogenic Escherichia coli infection	2/55	0.476	*ITGB1, TUBB3*
Sulfur metabolism	9/01	0.476	*PAPSS2*
Leishmaniasis	2/74	0.476	*ITGB1, TGFB3*
Pancreatic cancer	2/75	0.476	*TGFB3, CDKN2A*
Chronic myeloid leukemia	2/76	0.476	*TGFB3, CDKN2A*
Axon guidance	3/181	0.476	*SEMA6B, ITGB1, EPHA3*

Table 7: KEGG Pathway enrichment result for UF pattern of DEGs.

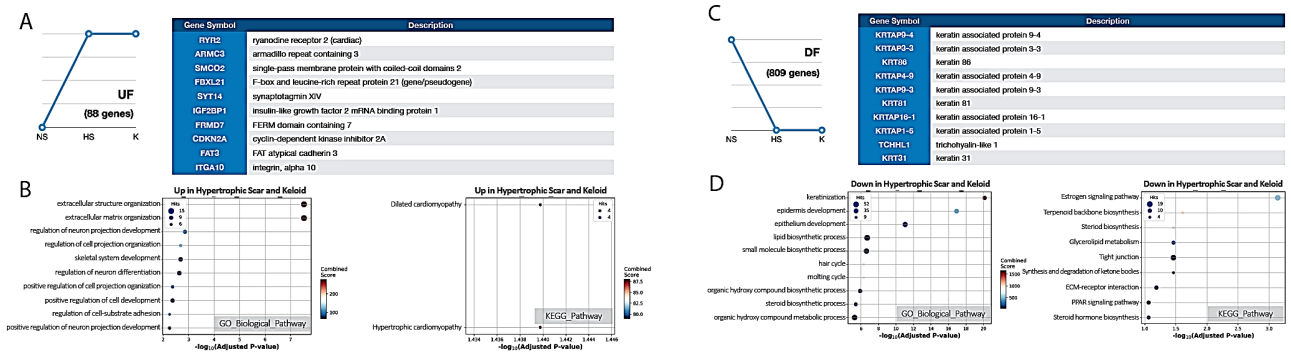

Figure 3: Differentially Expressed Genes (DEGs) specifically upregulated/downregulated in hypertrophic scars and keloids compared to normotrophic scars. A. DEGs in this group did not differ significantly between hypertrophic scars and keloids but were more upregulated than normotrophic scars. Among the 88 genes, RYR2 (ryanodine receptor 2), ARMC3 (armadillo repeat including 3), and SMCO2 (single-pass membrane protein with coiled-coil domains 2) are representative genes located in the upper rank; B. Genes associated with extracellular structural tissue and extracellular matrix tissues are commonly highly expressed in hypertrophic scars and keloids; C. Unlike the above analysis, DEGs in this group did not differ significantly between hypertrophic scars and keloids as in the previous group, but the expression was lower than that of normotrophic scars. It can be confirmed that almost all of the genes included in the upper rank among the 809 genes are keratin-associated proteins; D. And also it can be seen that they are related to keratinization through GO enrichment analysis.

GO ID	Term	Overlap	Adjusted P-value	Genes
GO:0031424	Keratinization	26/47	7.28E-21	*SPRR4, SPRR2E, SPRR2F, SPRR2G, TCHH, PPL, EVPL, LCE1A, LCE1B, LCE3D, CASP14, CDH3, SFN, SPRR2A, SPRR2B, TGM3, CNFN, LCE1F, LOR, LCE1C, LCE1D, LCE2B, KRT17, LCE6A, SPRR1A, IVL*
GO:0008544	Epidermis development	35/120	1.19E-17	*COL17A1, SPRR2E, SPRR2F, SPRR2G, CALML5, BNC1, KLK5, HOXC13, SOX21, EVPL, CST6, KLK7, KRT83, NTF4, CASP14, SOX9, SPRR2A, SPRR2B, DSP, WNT10A, LAMB3, KDF1, KRT34, KRT31, EDAR, ALDH3A2, LCE2B, DCT, KRT17, FABP5, KRT16, KRT15, KRT14, DNASE1L2, SPRR1A*
GO:0060429	Epithelium development	42/256	8.96E-12	*SPRR2E, RET, COL17A1, SPRR2F, SPRR2G, FOXC1, CALML5, SDC4, BNC1, KLK5, HOXC13, SOX21, EVPL, CST6, KLK7, KRT83, NTF4, CASP14, CECR2, EPCAM, SOX9, SPRR2A, SPRR2B, DSP, TFAP2B, WNT10A, LAMB3, KDF1, KRT34, KRT31, LCE2B, EDAR, ALDH3A2, BMP2, KRT17, FABP5, DCT, KRT16, KRT15, KRT14, DNASE1L2, SPRR1A*
GO:0008610	Lipid biosynthetic process	52/491	1.96E-07	*SLC44A5, PECR, TECR, MSMO1, TFCP2L1, PLB1, TM7SF2, FADS2, FADS6, SPTLC3, GGT1, GGT2, CERS4, DGAT2, EDN2, ELOVL4, HMGCS1, ACSL1, ELOVL3, CYP39A1, MVD, FAR2, SLC27A2, CFTR, CDS1, ACSS2, MVK, FAXDC2, INSIG1, ABHD5, HMGCR, CYP3A4, HSD17B8, AGPAT3, HSD11B1, HSD17B2, PIP5K1B, SPTSSB, SDR42E1, FDPS, PLA2G2D, GK, SRD5A1, DHCR24, ALOX15B, FABP5, GPAM, FASN, PNPLA3, DHCR7, DEGS2, LPIN3*
GO:0044283	Small molecule biosynthetic process	45/394	2.34E-07	*CDS1, SLC44A5, PECR, ACSS2, MVK, GLS2, FAXDC2, INSIG1, TECR, GPT, MSMO1, HMGCR, CYP3A4, HSD17B8, TM7SF2, FADS2, IMPA2, FADS6, KYNU, GGT1, GGT2, FDPS, EDN2, ELOVL4, PKLR, HMGCS1, GPT2, ELOVL3, BBOX1, DHCR24, UPB1, CYP4F12, ALOX15B, CYP39A1, GATM, BDH1, FABP5, FASN, PADI3, MVD, DHCR7, SLC27A2, CFTR, LPIN3, BCAT2*
GO:0042633	Hair cycle	9/15	5.09E-07	*KRT33B, KRTAP4-9, KRTAP4-8, KRTAP4-7, PPP1R13L, KRT16, KRT14, MPZL3, KRT83*
GO:0042303	Molting cycle	9/15	5.09E-07	*KRT33B, KRTAP4-9, KRTAP4-8, KRTAP4-7, PPP1R13L, KRT16, KRT14, MPZL3, KRT83*
GO:1901617	Organic hydroxy compound biosynthetic process	26/166	1.24E-06	*CDS1, SLC44A5, PMEL, OCA2, MVK, INSIG1, TYRP1, MSMO1, HMGCR, CYP3A4, TM7SF2, IMPA2, FDPS, GPR37, HMGCS1, BBOX1, DHCR24, TYR, CYP39A1, DCT, FABP5, MVD, DHCR7, SLC27A2, CFTR, LPIN3*
GO:0006694	Steroid biosynthetic process	20/108	3.94E-06	*SDR42E1, FDPS, MVK, HMGCS1, SRD5A1, INSIG1, MSMO1, DHCR24, TFCP2L1, HMGCR, CYP3A4, HSD17B8, TM7SF2, CYP39A1, HSD11B1, HSD17B2, MVD, DHCR7, SLC27A2, CFTR*
GO:1901615	Organic hydroxy compound metabolic process	47/476	5.41E-06	*CDS1, SLC44A5, OCA2, PECR, CEBPA, PMEL, ACSS2, MVK, FOXE1, INSIG1, TYRP1, GDPD2, MSMO1, HMGCR, CYP3A4, PLB1, TM7SF2, SDR16C5, PPIP5K1, IMPA2, AWAT2, LRAT, FDPS, PLA2G2D, GPR37, DGAT2, GK, HMGCS1, SORD, BBOX1, DHCR24, TYR, CYP4F12, CYP39A1, ALDH3A2, AKR1B10, FABP5, SOAT1, DCT, PLCH1, MVD, DHCR7, DEGS2, SLC27A2, GPLD1, CFTR, LPIN3*

Table 8: GO Biological Process enrichment result for DF pattern of DEGs.

Term	Overlap	Adjusted P-value	Genes
Estrogen signaling pathway	19/137	0.000726	*CALML5, TGFA, KRT23, KRT34, CALML3, KRT31, ESR1, KRT33B, KRT33A, KRT18, KRT39, KRT17, KRT16, KRT26, KRT15, KRT36, KRT14, PGR, FKBP5*
Terpenoid backbone biosynthesis	6/22	0.0246	*FDPS, MVK, HMGCS1, MVD, HMGCR, ACAT2*
Steroid biosynthesis	5/19	0.0346	*SOAT1, DHCR24, MSMO1, DHCR7, TM7SF2*
Glycerolipid metabolism	9/61	0.0346	*ALDH3A2, DGAT2, AKR1B10, GK, GPAM, PNPLA3, PNLIPRP3, AGPAT3, LPIN3*
Tight junction	17/170	0.0346	*MAP3K1, F11R, PRKCZ, CD1A, TIAM1, SLC9A3R1, EPB41L4B, OCLN, CLDN3, MARVELD2, PPP2R2C, CLDN16, EZR, CFTR, LLGL2, TJP2, CRB3*
Synthesis and degradation of ketone bodies	10/04	0.0346	*BDH1, HMGCS1, OXCT2, ACAT2*
ECM-receptor interaction	10/82	0.0653	*SDC4, LAMB3, LAMC3, ITGB4, ITGA2, LAMB4, COL4A6, COL4A5, ITGB6, GP6*
PPAR signaling pathway	9/74	0.0868	*FADS2, GK, FABP5, ACSL1, FABP7, ME1, SLC27A6, ACSBG1, SLC27A2*
Steroid hormone biosynthesis	8/60	0.0868	*SULT2B1, HSD11B1, SULT1E1, SRD5A1, HSD17B2, UGT1A4, CYP3A4, HSD17B8*
Pyruvate metabolism	6/39	0.118	*ALDH3A2, ACSS2, PC, PKLR, ME1, ACAT2*

Table 9: KEGG Pathway enrichment result for DF pattern of DEGs.

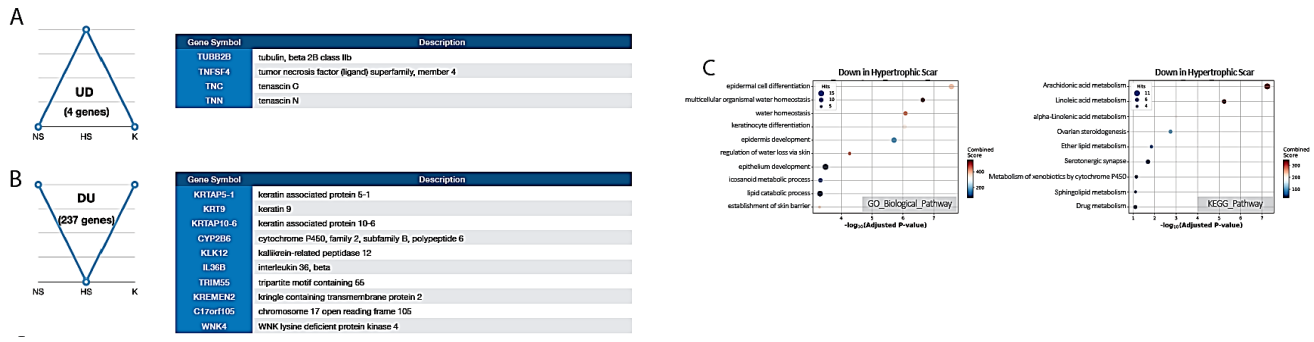

Figure 4: Differentially Expressed Genes (DEGs) specific to hypertrophic scars compared to normotrophic scars and keloids. A. The number of DEGs especially upregulated in hypertrophic scars than in normotrophic scars and keloids, is four, which is TUBB2B (tubulin, beta 2B class IIb), TNFSF4 (tumor necrosis factor superfamily, member 4), TNC (tenascin C), TNN (tenascin N); B. A total of 237 DEGs specifically downregulated only in hypertrophic scars. As the top-ranked genes, KRTAP5-1 (keratin associated protein 5-1), KRT9 (keratin9), and KRTAP10-6 (keratin associated protein 10-6) are commonly related to keratin; C. DEGs highly downregulated in hypertrophic scars are related to epidermal cell differentiation and water homeostasis. In addition, arachidonic acid metabolism and linoleic acid metabolism were ranked high in the KEGG pathway enrichment analysis.

GO ID	Term	Overlap	Adjusted P-value	Genes
GO:0009913	Epidermal cell differentiation	13/76	2.68E-08	*CERS3, CSTA, CDSN, SPINK5, OVOL1, POU2F3, FOXN1, TGM1, SCEL, FA2H, ACER1, IRF6, TP63*
GO:0050891	Multicellular organismal water homeostasis	9/32	2.27E-07	*CDH1, CYP4F2, SCNN1B, SCNN1A, ALOX12B, ABCA12, CLDN1, ALOXE3, TP63*
GO:0030104	Water homeostasis	9/38	8.28E-07	*CDH1, CYP4F2, SCNN1B, SCNN1A, ALOX12B, ABCA12, CLDN1, ALOXE3, TP63*
GO:0030216	Keratinocyte differentiation	10/54	8.88E-07	*TGM1, CERS3, SCEL, ACER1, CSTA, CDSN, IRF6, POU2F3, FOXN1, TP63*
GO:0008544	Epidermis development	13/120	1.94E-06	*TFAP2C, CDSN, GRHL3, KRT5, FOXN1, POU2F3, KRT9, ACER1, SCEL, GJB5, TGM5, SPRR2D, ZNF750*
GO:0033561	Regulation of water loss via skin	6/19	5.36E-05	*CDH1, ALOX12B, ABCA12, CLDN1, ALOXE3, TP63*
GO:0060429	Epithelium development	15/256	0.000325	*TFAP2C, CDSN, GRHL3, KRT5, GATA3, FOXN1, POU2F3, KRT9, ACER1, SCEL, GJB5, TGM5, FGFR3, SPRR2D, ZNF750*
GO:0006690	Icosanoid metabolic process	9/88	0.000473	*CYP2J2;CYP2C9;PLA2G4F;GGT6;PLA2G4B;CYP4F2;CYP4F3; ALOX12B;ALOXE3*
GO:0016042	Lipid catabolic process	14/232	0.000488	*PLA2G2F, PLA2G4F, PLA2G4D, PLA2G4E, CYP4F2, PLA2G4B, CYP4F3, SMPD3, ACER1, LIPH, LIPM, LIPK, PLCH2, PNPLA1*
GO:0061436	Establishment of skin barrier	5/16	0.000507	*ALOX12B, ABCA12, CLDN1, ALOXE3, TP63*

Table 10: GO Biological Process enrichment result for DU pattern of DEGs.

Term	Overlap	Adjusted P-value	Genes
Arachidonic acid metabolism	11/63	5.66E-08	*PLA2G2F, CYP2J2, CYP2C9, PLA2G4F, CYP2B6, PLA2G4D, PLA2G4E, PLA2G4B, CYP4F2, CYP4F3, ALOX12B*
Linoleic acid metabolism	7/29	5.78E-06	*PLA2G2F, CYP2J2, CYP2C9, PLA2G4F, PLA2G4D, PLA2G4E, PLA2G4B*
alpha-Linolenic acid metabolism	5/25	0.00101	*PLA2G2F, PLA2G4F, PLA2G4D, PLA2G4E, PLA2G4B*
Ovarian steroidogenesis	6/49	0.00183	*CYP2J2, PLA2G4F, PLA2G4D, STAR, PLA2G4E, PLA2G4B*
Ether lipid metabolism	5/47	0.0141	*PLA2G2F, PLA2G4F, PLA2G4D, PLA2G4E, PLA2G4B*
Serotonergic synapse	7/113	0.0205	*CYP2J2, CYP2C9, PLA2G4F, PLA2G4D, PLA2G4E, PLA2G4B, ALOX12B*
Metabolism of xenobiotics by cytochrome P450	5/74	0.0715	*ALDH3B2, CYP2C9, CYP2B6, GSTA3, UGT1A6*
Sphingolipid metabolism	4/47	0.0787	*SMPD3, CERS3, ACER1, SGPP2*
Drug metabolism	6/108	0.0801	*ALDH3B2, CYP2C9, CYP2B6, GSTA3, XDH, UGT1A6*
VEGF signaling pathway	4/59	0.162	*PLA2G4F, PLA2G4D, PLA2G4E, PLA2G4B*

Table 11: KEGG Pathway enrichment result for DU pattern of DEGs.

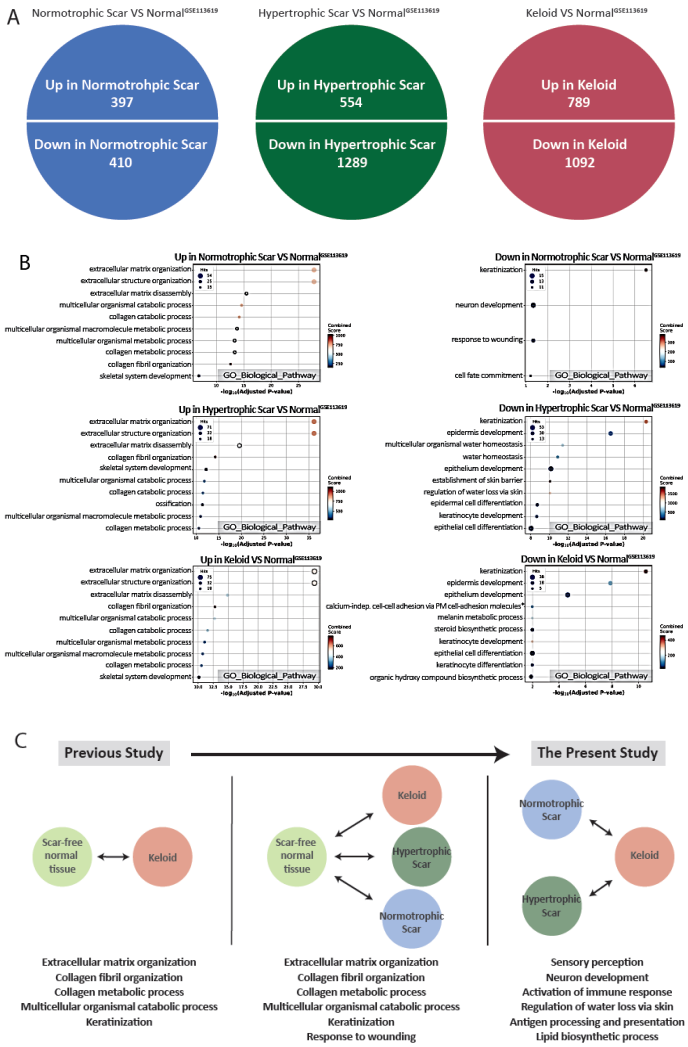

Figure 5: Normotrophic scar, rather than scar free normal skin is ideal for the identification of scar specific DEGs. A. Comparing gene expression profile of normotrophic scars, hypertrophic scars and keloids from the current study against scar free normal skin sample obtained from public database GSE113619; B. Compared with scar free normal skin, the upregulated DEGs in normotrophic scars, hypertrophic scars and keloids respectively overlap. Genes related to extracellular matrix organization, extracellular structure organization and extracellular matrix disassembly were commonly upregulated in DEGs of three scar tissues compared to scar free normal skin. Conversely, DEGs commonly downregulated in each scar tissue are keratinization and epithelial cell differentiation; C. A figure explaining the novelty of the new research strategy, along with the limitations of previous research and the existing research method.

GO ID	Term	Overlap	Adjusted P-value	Genes
GO:0030198	Extracellular matrix organization	54/359	1.44E-28	*COL14A1, SERPINE1, COL12A1, CYR61, LOXL2, COMP, EFEMP2, ADAMTS2, IBSP, COL10A1, POSTN, EGFL6, MMP1, MMP2, MMP3, FGG, BGN, ADAMTS20, MMP11, VCAN, SFRP2, COL2A1, MMP13, COL4A1, COL6A2, PXDN, COL6A1, COL6A3, MATN3, ENG, FBN2, FOXC2, LAMA2, COL11A1, KLK4, LTBP3, NID2, ACAN, ADAMTS14, ABI3BP, SPP1, TGFB3, FN1, SULF1, SULF2, DSPP, COL1A1, COL1A2, COL5A1, ITGA10, COL5A2, MFAP2, COL20A1, FBN1*
GO:0043062	Extracellular structure organization	54/360	1.44E-28	*COL14A1, SERPINE1, COL12A1, CYR61, LOXL2, COMP, EFEMP2, ADAMTS2, IBSP, COL10A1, POSTN, EGFL6, MMP1, MMP2, MMP3, FGG, BGN, ADAMTS20, MMP11, VCAN, SFRP2, COL2A1, MMP13, COL4A1, COL6A2, PXDN, COL6A1, COL6A3, MATN3, ENG, FBN2, FOXC2, LAMA2, COL11A1, KLK4, LTBP3, NID2, ACAN, ADAMTS14, ABI3BP, SPP1, TGFB3, FN1, SULF1, SULF2, DSPP, COL1A1, COL1A2, COL5A1, ITGA10, COL5A2, MFAP2, COL20A1, FBN1*
GO:0022617	Extracellular matrix disassembly	25/116	3.48E-16	*FBN2, COL14A1, COL11A1, COL12A1, KLK4, ACAN, SPP1, COL10A1, MMP1, MMP2, MMP3, FN1, COL1A1, MMP11, COL1A2, COL2A1, MMP13, COL5A1, COL4A1, COL6A2, COL5A2, COL6A1, COL6A3, FBN1, ENG*
GO:0044243	Multicellular organismal catabolic process	21/80	2.35E-15	*ACE, COL14A1, MMP1, MMP2, COL11A1, COL12A1, MMP3, COL1A1, MMP11, ADAMTS2, ADAMTS14, MMP13, COL2A1, COL1A2, COL5A1, COL4A1, COL6A2, COL6A1, COL5A2, COL10A1, COL6A3*
GO:0030574	Collagen catabolic process	20/74	6.36E-15	*COL14A1, MMP1, MMP2, COL11A1, COL12A1, MMP3, COL1A1, MMP11, ADAMTS2, ADAMTS14, MMP13, COL2A1, COL1A2, COL5A1, COL4A1, COL6A2, COL6A1, COL5A2, COL10A1, COL6A3*
GO:0044259	Multicellular organismal macromolecule metabolic process	21/89	1.72E-14	*ACE, COL14A1, MMP1, MMP2, COL11A1, COL12A1, MMP3, COL1A1, MMP11, ADAMTS2, ADAMTS14, MMP13, COL2A1, COL1A2, COL5A1, COL4A1, COL6A2, COL6A1, COL5A2, COL10A1, COL6A3*
GO:0044236	Multicellular organismal metabolic process	21/94	4.69E-14	*ACE, COL14A1, MMP1, MMP2, COL11A1, COL12A1, MMP3, COL1A1, MMP11, ADAMTS2, ADAMTS14, MMP13, COL2A1, COL1A2, COL5A1, COL4A1, COL6A2, COL6A1, COL5A2, COL10A1, COL6A3*
GO:0032963	Collagen metabolic process	20/83	4.69E-14	*COL14A1, MMP1, MMP2, COL11A1, COL12A1, MMP3, COL1A1, MMP11, ADAMTS2, ADAMTS14, MMP13, COL2A1, COL1A2, COL5A1, COL4A1, COL6A2, COL6A1, COL5A2, COL10A1, COL6A3*
GO:0030199	Collagen fibril organization	15/41	2.55E-13	*FOXC2, COL14A1, COL11A1, COL12A1, LOXL2, COL1A1, ACAN, MMP11, ADAMTS14, ADAMTS2, COL1A2, COL2A1, SFRP2, COL5A1, COL5A2*
GO:0001501	Skeletal system development	19/162	1.49E-07	*POSTN, COL12A1, IGF2, AEBP1, SULF1, PAPSS2, PAX1, SULF2, DSPP, COMP, COL1A1, ACAN, COL1A2, COL2A1, COL5A2, COL10A1, ARSE, MATN3, FBN1*

Table 12: GO Biological Process enrichment result for up regulated DEGs in Normotrophic Scar VS. Normal (GSE113619).

GO ID	Term	Overlap	Adjusted P-value	Genes
GO:0031424	Keratinization	12/47	3.08E-07	*LCE1A, LCE2B, LCE1B, LCE4A, LCE6A, LCE1E, EVPL, LCE1F, LCE2D, LOR, LCE1C, LCE1D*
GO:0030182	Neuron differentiation	15/222	0.0461	*BCL11B, WNT3A, WNT7B, WNT9B, WNT7A, RORA, WNT16, GDF7, NTF4, NGRN, ID4, FGFR3, WNT3, HES5, WNT4*
GO:0009611	Response to wounding	13/167	0.0461	*SERPINB2, PLLP, TGFA, NMNAT3, KLK8, POU2F3, EREG, RTN4RL1, CYP1A1, BCL2, TSPO, FGFR3, MATN4*
GO:0045165	Cell fate commitment	11/134	0.0608	*WNT3A, WNT7B, BCL2, WNT9B, WNT7A, WNT16, FGFR3, WNT3, HES5, WNT4, GDF7*
GO:0060429	Epithelium development	15/256	0.131	*CALML5, SDC4, WNT7B, KDF1, KLK5, FOXJ1, EVPL, POU2F3, POU3F3, LCE2B, NTF4, FGFR3, WNT3, HES5, WNT4*
GO:0035588	G-protein coupled purinergic receptor signaling pathway	4/17	0.131	*ADORA2A, P2RY2, P2RY1, ADORA1*
GO:0061098	Positive regulation of protein tyrosine kinase activity	5/32	0.131	*WNT3A, DOK7, ADORA1, TGFA, EREG*
GO:0014014	Negative regulation of gliogenesis	5/32	0.131	*ID4, TSPO, ASCL2, FGFR3, HES5*
GO:0022010	Central nervous system myelination	9/03	0.131	*ID4, FGFR3, HES5*
GO:0060428	Lung epithelium development	9/03	0.131	*WNT7B, FOXJ1, FGFR3*

Table 13: GO Biological Process enrichment result for down regulated DEGs in Normotrophic Scar VS Normal (GSE113619).

GO ID	Term	Overlap	Adjusted P-value	Genes
GO:0030198	Extracellular matrix organization	71/359	8.08E-37	*OLFML2B, COL14A1, ELN, SERPINE1, COL12A1, TNC, SCX, PLOD2, PLOD1, CYR61, LOXL2, COMP, ADAMTS4, EFEMP2, ADAMTS2, IBSP, SH3PXD2B, COL10A1, POSTN, EGFL6, MMP2, BGN, HSPG2, ADAMTS20, MMP11, VCAN, SFRP2, COL2A1, MMP13, COL4A1, COL6A2, PXDN, COL6A1, COL8A1, COL6A3, MATN3, ENG, FBN2, FOXC2, LAMA2, COL11A1, LAMA4, KLK4, LTBP3, NID2, ACAN, ADAMTS14, ABI3BP, SPP1, TGFB1, COL24A1, TGFB3, LUM, FN1, LAMB1, SULF1, GDF5, SULF2, DSPP, COL1A1, COL3A1, COL1A2, BMP1, COL5A1, WT1, ITGA10, COL5A2, ITGA11, MFAP2, TLL2, FBN1*
GO:0043062	Extracellular structure organization	71/360	8.08E-37	*OLFML2B, COL14A1, ELN, SERPINE1, COL12A1, TNC, SCX, PLOD2, PLOD1, CYR61, LOXL2, COMP, ADAMTS4, EFEMP2, ADAMTS2, IBSP, SH3PXD2B, COL10A1, POSTN, EGFL6, MMP2, BGN, HSPG2, ADAMTS20, MMP11, VCAN, SFRP2, COL2A1, MMP13, COL4A1, COL6A2, PXDN, COL6A1, COL8A1, COL6A3, MATN3, ENG, FBN2, FOXC2, LAMA2, COL11A1, LAMA4, KLK4, LTBP3, NID2, ACAN, ADAMTS14, ABI3BP, SPP1, TGFB1, COL24A1, TGFB3, LUM, FN1, LAMB1, SULF1, GDF5, SULF2, DSPP, COL1A1, COL3A1, COL1A2, BMP1, COL5A1, WT1, ITGA10, COL5A2, ITGA11, MFAP2, TLL2, FBN1*
GO:0022617	Extracellular matrix disassembly	32/116	2.68E-20	*FBN2, COL14A1, ELN, COL11A1, COL12A1, KLK4, ADAMTS4, ACAN, SH3PXD2B, SPP1, COL10A1, MMP2, FN1, LAMB1, HSPG2, COL1A1, MMP11, COL3A1, COL1A2, BMP1, COL2A1, MMP13, COL5A1, COL4A1, COL6A2, COL5A2, COL6A1, COL8A1, COL6A3, TLL2, FBN1, ENG*
GO:0030199	Collagen fibril organization	18/41	5.93E-15	*FOXC2, COL14A1, LUM, COL11A1, COL12A1, SCX, LOXL2, COL1A1, ACAN, MMP11, ADAMTS14, ADAMTS2, COL3A1, COL1A2, COL2A1, SFRP2, COL5A1, COL5A2*
GO:0001501	Skeletal system development	29/162	6.02E-13	*HOXD1, COL12A1, SCX, AEBP1, PHEX, PAPSS2, COMP, ADAMTS4, ACAN, SH3PXD2B, COL10A1, ARSE, POSTN, DMRT2, IGF2, SULF1, PAX1, SULF2, DSPP, COL1A1, COL3A1, COL1A2, BMP1, COL2A1, COL5A2, CDH11, ALPL, MATN3, FBN1*
GO:0044243	Multicellular organismal catabolic process	21/80	1.50E-12	*ACE, COL14A1, MMP2, COL11A1, COL12A1, COL1A1, MMP11, ADAMTS2, ADAMTS14, COL3A1, MMP13, COL2A1, COL1A2, COL5A1, COL4A1, COL6A2, COL6A1, COL5A2, COL10A1, COL8A1, COL6A3*
GO:0030574	Collagen catabolic process	20/74	3.19E-12	*COL14A1, MMP2, COL11A1, COL12A1, COL1A1, MMP11, ADAMTS2, ADAMTS14, COL3A1, MMP13, COL2A1, COL1A2, COL5A1, COL4A1, COL6A2, COL6A1, COL5A2, COL10A1, COL8A1, COL6A3*
GO:0001503	Ossification	24/116	3.93E-12	*FOXC2, ECM1, TGFB1, TGFB3, MMP2, BMP8A, SCX, CHRDL2, HSPG2, RUNX2, CTGF, DSPP, COL1A1, IGSF10, MN1, BMP1, COL2A1, MMP13, CDH11, GNAS, SPP1, ALPL, COL10A1, CTHRC1*
GO:0044259	Multicellular organismal macromolecule metabolic process	21/89	1.02E-11	*ACE, COL14A1, MMP2, COL11A1, COL12A1, COL1A1, MMP11, ADAMTS2, ADAMTS14, COL3A1, MMP13, COL2A1, COL1A2, COL5A1, COL4A1, COL6A2, COL6A1, COL5A2, COL10A1, COL8A1, COL6A3*
GO:0032963	Collagen metabolic process	20/83	2.46E-11	*COL14A1, MMP2, COL11A1, COL12A1, COL1A1, MMP11, ADAMTS2, ADAMTS14, COL3A1, MMP13, COL2A1, COL1A2, COL5A1, COL4A1, COL6A2, COL6A1, COL5A2, COL10A1, COL8A1, COL6A3*

Table 14: GO Biological Process enrichment result for up regulated DEGs in Hypertrophic Scar VS. Normal (GSE113619).

GO ID	Term	Overlap	Adjusted P-value	Genes
GO:0031424	Keratinization	30/47	4.70E-21	*SPRR2E, ABCA12, PPL, EVPL, LCE2D, TGM1, LCE1A, LCE1B, LCE3D, CASP14, LCE5A, SFN, TGM3, SPRR2D, KRT2, CNFN, LCE1E, LCE1F, LOR, LCE1C, LCE3E, LCE1D, LCE2B, LCE2C, LCE2A, KRT17, LCE4A, LCE6A, SPRR1B, IVL*
GO:0008544	Epidermis development	42/120	2.90E-17	*COL17A1, SPRR2E, CALML5, BNC1, KLK5, HOXC13, SOX21, EVPL, CST6, KLK7, NTF4, CASP14, SCEL, ALX4, TGM5, SPRR2D, DSP, TFAP2C, WNT10A, CDSN, LAMB3, KRT2, KDF1, GRHL3, KRT5, KRT31, FOXN1, POU2F3, KRT9, EDAR, LCE2B, ACER1, ELF3, DCT, KRT17, KRT16, KRT15, GJB5, KRT14, DNASE1L2, SPRR1B, ZNF750*
GO:0050891	Multicellular organismal water homeostasis	19/32	3.93E-12	*FLG, CYP4F2, KRT1, KDF1, ALOX12B, ALOX12, ABCA12, CLDN1, CYP4F12, FLG2, SCNN1G, CLDN4, CDH1, SCNN1B, TMEM79, SCNN1A, SFN, ALOXE3, TP63*
GO:0030104	Water homeostasis	20/38	1.32E-11	*FLG, CYP4F2, AQP9, KRT1, KDF1, ALOX12B, ALOX12, ABCA12, CLDN1, CYP4F12, FLG2, SCNN1G, CLDN4, CDH1, SCNN1B, TMEM79, SCNN1A, SFN, ALOXE3, TP63*
GO:0060429	Epithelium development	52/256	7.04E-11	*CALML5, BNC1, HOXC13, SOX21, CASP14, TGM5, DSP, KRT2, KRT5, KRT31, POU3F3, KRT9, LCE2B, EDAR, SFRP1, ELF3, DCT, DNASE1L2, ZNF750, SPRR2E, COL17A1, SDC4, KLK5, GATA3, EVPL, CST6, KLK7, NTF4, SCEL, ALX4, WNT3, HES5, SPRR2D, WNT4, WNT10A, TFAP2C, CDSN, LAMB3, WNT7B, KDF1, FOXJ1, GRHL3, FOXN1, POU2F3, ACER1, KRT17, KRT16, KRT15, GJB5, KRT14, FGFR3, SPRR1B*

GO:0061436	Establishment of skin barrier	13/16	8.84E-11	*FLG, KRT1, KDF1, ALOX12B, ALOX12, ABCA12, CLDN1, FLG2, CLDN4, TMEM79, SFN, ALOXE3, TP63*
GO:0033561	Regulation of water loss via skin	14/19	8.87E-11	*FLG, KRT1, KDF1, ALOX12B, ALOX12, ABCA12, CLDN1, FLG2, CLDN4, CDH1, TMEM79, SFN, ALOXE3, TP63*
GO:0009913	Epidermal cell differentiation	25/76	1.99E-09	*FLG, CSTA, EVPL, TGM1, SCEL, TGM3, TP63, HES5, DSP, CERS3, ST14, CDSN, SPINK5, KRT10, POU3F1, OVOL1, POU2F3, FOXN1, LOR, EREG, FA2H, ACER1, IRF6, IVL, SPRR1B*
GO:0030216	Keratinocyte differentiation	21/54	2.27E-09	*DSP, CERS3, FLG, CSTA, ST14, CDSN, KRT10, POU3F1, EVPL, POU2F3, FOXN1, LOR, EREG, TGM1, SCEL, ACER1, IRF6, TGM3, TP63, IVL, SPRR1B*
GO:0030855	Epithelial cell differentiation	53/303	9.18E-09	*EHF, CTSV, F11R, SYNE4, TGM1, UPK1B, TP63, TGM3, CERS3, DSP, CBR1, MREG, KRT4, TCF15, SPINK5, OVOL1, POU3F1, KLF15, LOR, EREG, ELF3, TST, ELF5, ALDOC, IRF6, RHCG, IVL, FLG, OCA2, CSTA, DLX3, TYRP1, EVPL, SCEL, AGR2, HES5, SPDEF, WNT4, ST14, CDSN, PTK6, KRT10, FOXN1, POU2F3, GDF7, FA2H, ACER1, KRT16, KRT14, CYP1A1, BCL2, CD24, SPRR1B*

Table 15: GO Biological Process enrichment result for down regulated DEGs in Hypertrophic Scar VS. Normal (GSE113619).

GO ID	Term	Overlap	Adjusted P-value	Genes
GO:0030198	Extracellular matrix organization	75/359	4.56E-30	*COL16A1, OLFML2B, COL14A1, SERPINE1, COL12A1, SCX, PLOD2, PLOD1, CYR61, LOXL2, COMP, ADAMTS4, EFEMP2, ADAMTS2, IBSP, SH3PXD2B, COL10A1, FGA, POSTN, COL27A1, EGFL6, MMP2, BGN, HSPG2, ADAMTS20, MMP11, VCAN, SFRP2, COL2A1, MMP13, COL6A2, PXDN, COL6A1, COL8A1, COL6A3, COL6A6, MATN3, ENG, FBN2, FOXC2, LAMA1, COL11A1, COL11A2, KLK4, LTBP3, NID2, ACAN, ADAMTS14, ABI3BP, TGFB1, COL24A1, FOXF2, FOXF1, TGFB3, LUM, FN1, SULF1, GDF5, AGT, SULF2, DSPP, COL1A1, COL3A1, COL1A2, BMP1, COL5A1, NPHS1, ITGA10, COL5A2, ITGA11, MFAP2, COL9A1, COL20A1, TLL2, FBN1*
GO:0043062	Extracellular structure organization	75/360	4.56E-30	*COL16A1, OLFML2B, COL14A1, SERPINE1, COL12A1, SCX, PLOD2, PLOD1, CYR61, LOXL2, COMP, ADAMTS4, EFEMP2, ADAMTS2, IBSP, SH3PXD2B, COL10A1, FGA, POSTN, COL27A1, EGFL6, MMP2, BGN, HSPG2, ADAMTS20, MMP11, VCAN, SFRP2, COL2A1, MMP13, COL6A2, PXDN, COL6A1, COL8A1, COL6A3, COL6A6, MATN3, ENG, FBN2, FOXC2, LAMA1, COL11A1, COL11A2, KLK4, LTBP3, NID2, ACAN, ADAMTS14, ABI3BP, TGFB1, COL24A1, FOXF2, FOXF1, TGFB3, LUM, FN1, SULF1, GDF5, AGT, SULF2, DSPP, COL1A1, COL3A1, COL1A2, BMP1, COL5A1, NPHS1, ITGA10, COL5A2, ITGA11, MFAP2, COL9A1, COL20A1, TLL2, FBN1*
GO:0022617	Extracellular matrix disassembly	32/116	1.23E-15	*FBN2, COL16A1, COL14A1, COL11A1, COL12A1, COL11A2, KLK4, ADAMTS4, ACAN, SH3PXD2B, COL10A1, MMP2, FN1, HSPG2, COL1A1, MMP11, COL3A1, COL1A2, BMP1, COL2A1, MMP13, COL5A1, COL6A2, COL5A2, COL6A1, COL9A1, COL8A1, COL6A3, TLL2, COL6A6, FBN1, ENG*
GO:0030199	Collagen fibril organization	19/41	1.59E-13	*FOXC2, COL14A1, LUM, COL11A1, COL12A1, COL11A2, SCX, LOXL2, COL1A1, ACAN, MMP11, ADAMTS14, ADAMTS2, COL3A1, COL1A2, COL2A1, SFRP2, COL5A1, COL5A2*
GO:0044243	Multicellular organismal catabolic process	25/80	1.76E-13	*COL16A1, COL14A1, PLA2G1B, COL11A1, COL12A1, COL11A2, ADAMTS2, ADAMTS14, COL10A1, ACE, MMP2, COL1A1, MMP11, COL3A1, MMP13, COL2A1, COL1A2, COL5A1, COL6A2, COL6A1, COL5A2, COL9A1, COL8A1, COL6A3, COL6A6*
GO:0030574	Collagen catabolic process	23/74	2.63E-12	*COL16A1, COL14A1, MMP2, COL11A1, COL12A1, COL11A2, COL1A1, MMP11, ADAMTS2, ADAMTS14, COL3A1, MMP13, COL2A1, COL1A2, COL5A1, COL6A2, COL6A1, COL5A2, COL9A1, COL10A1, COL8A1, COL6A3, COL6A6*
GO:0044236	Multicellular organismal metabolic process	25/94	8.37E-12	*COL16A1, COL14A1, PLA2G1B, COL11A1, COL12A1, COL11A2, ADAMTS2, ADAMTS14, COL10A1, ACE, MMP2, COL1A1, MMP11, COL3A1, MMP13, COL2A1, COL1A2, COL5A1, COL6A2, COL6A1, COL5A2, COL9A1, COL8A1, COL6A3, COL6A6*
GO:0044259	Multicellular organismal macromolecule metabolic process	24/89	1.75E-11	*COL16A1, ACE, COL14A1, MMP2, COL11A1, COL12A1, COL11A2, COL1A1, MMP11, ADAMTS2, ADAMTS14, COL3A1, MMP13, COL2A1, COL1A2, COL5A1, COL6A2, COL6A1, COL5A2, COL9A1, COL10A1, COL8A1, COL6A3, COL6A6*
GO:0032963	Collagen metabolic process	23/83	2.79E-11	*COL16A1, COL14A1, MMP2, COL11A1, COL12A1, COL11A2, COL1A1, MMP11, ADAMTS2, ADAMTS14, COL3A1, MMP13, COL2A1, COL1A2, COL5A1, COL6A2, COL6A1, COL5A2, COL9A1, COL10A1, COL8A1, COL6A3, COL6A6*
GO:0001501	Skeletal system development	31/162	7.58E-11	*HOXD1, COL12A1, COL11A2, SCX, AEBP1, PHEX, PAPSS2, GLI2, COMP, ADAMTS4, RAI1, ACAN, SH3PXD2B, COL10A1, SPP2, ARSE, POSTN, IGF2, SULF1, PAX1, SULF2, DSPP, COL1A1, COL3A1, COL1A2, BMP1, COL2A1, COL5A2, CDH11, MATN3, FBN1*

Table 16: GO Biological Process enrichment result for up regulated DEGs in Keloid VS. Normal (GSE113619).

GO ID	Term	Overlap	Adjusted P-value	Genes
GO:0031424	Keratinization	21/47	2.80E-11	*KRT2, CNFN, LCE1E, PPL, EVPL, LCE1F, LCE2D, LOR, LCE1C, LCE3E, LCE1D, LCE1A, LCE2B, LCE1B, LCE2C, LCE2A, LCE5A, LCE4A, LCE6A, SFN, TGM3*
GO:0008544	Epidermis development	29/120	1.33E-08	*COL17A1, CALML5, BNC1, KLK5, SOX21, EVPL, CST6, KLK7, NTF4, SCEL, TGM5, DSP, TFAP2C, WNT10A, LAMB3, KRT2, KDF1, GRHL3, KRT5, POU2F3, EDAR, LCE2B, ACER1, ELF3, DCT, KRT15, GJB5, KRT14, DNASE1L2*
GO:0060429	Epithelium development	38/256	2.21E-05	*COL17A1, CALML5, SDC4, BNC1, KLK5, SOX21, EVPL, CST6, KLK7, NTF4, SCEL, TGM5, WNT3, HES5, WNT4, DSP, WNT10A, TFAP2C, LAMB3, KRT2, KDF1, FOXJ1, GRHL3, KRT5, POU2F3, POU3F3, LCE2B, EDAR, ACER1, SFRP1, ELF3, DCT, KRT15, GJB5, KRT14, SDC1, DNASE1L2, FGFR3*
GO:0016338	Calcium-independent cell-cell adhesion via plasma membrane cell-adhesion molecules	8/22	0.0103	*CLDN10, CLDN4, CLDN3, CLDN8, CLDN23, CLDN7, CLDN16, CLDN1*
GO:0006582	Melanin metabolic process	12/06	0.0103	*PMEL, DCT, TYRP1, ASIP, BCL2, TYR*
GO:0006694	Steroid biosynthetic process	18/108	0.0103	*SDR42E1, HMGCS1, SRD5A1, DHCR24, TFCP2L1, HSD17B8, TM7SF2, CYP39A1, HSD11B1, CYB5R1, STAR, HSD17B1, TSPO, MVD, DHCR7, HMGCS2, SLC27A2, WNT4*
GO:0003334	Keratinocyte development	8/05	0.0103	*TFAP2C, BCL11B, KDF1, SFN, EXPH5*
GO:0030855	Epithelial cell differentiation	35/303	0.0103	*EHF, DLX3, TYRP1, CTSV, F11R, EVPL, SCEL, TGM3, HES5, SPDEF, WNT4, CERS3, DSP, CBR1, ST14, MREG, PTK6, OVOL1, POU3F1, POU2F3, KLF15, LOR, EREG, GDF7, ACER1, DHRS9, ELF3, TST, ELF5, KRT14, BCL2, ALDOC, IRF6, CD24, RHCG*
GO:0030216	Keratinocyte differentiation	12/54	0.0103	*DSP, CERS3, SCEL, ACER1, ST14, IRF6, POU3F1, EVPL, POU2F3, TGM3, LOR, EREG*
GO:1901617	Organic hydroxy compound biosynthetic process	23/166	0.0126	*CDS1, PMEL, GPR37, HMGCS1, TYRP1, ASIP, BBOX1, ALOX12, DHCR24, TYR, TM7SF2, CYP39A1, CYB5R1, ACER1, STAR, DCT, IMPA2, HSD17B1, LEP, MVD, DHCR7, HMGCS2, SLC27A2*

Table 17: GO Biological Process enrichment result for down regulated DEGs in Keloid VS. Normal (GSE113619).

Discussion

In this study, to identify keloid-specific gene expression profiles, keloid tissues were compared with reversible scar tissues using whole transcriptome analysis. In addition, hypertrophic scar-specific genes were determined. Our present study suggests that peripheral development and immune regulation-related genes are involved in the pathogenesis of keloids. To the best of our knowledge, no such results have been reported previously.

The wound repair process has several phases: The (1) inflammatory phase, (2) proliferative phase, and (3) remodeling phase [31-33]. In the first step, activation of platelets and the clotting cascade cause blood clotting and immobilization of platelets at the wound site. Then inflammatory cells are recruited to the wound site. During the proliferation phase, fibroblasts are activated and differentiated into myofibroblast-producing and organizing ECM molecules, activating the process of re-epithelialization. Finally, during the remodeling (maturation) phase, collagen fibers are remodeled, and excessive fibroblasts are removed by apoptosis.

We confirmed that the expression of genes related to extracellular matrix organization and disassembly was highly expressed in hypertrophic scars and keloids compared to scar free normal skin tissue based on the analysis of GO biological process and KEGG pathway, as well as elevated expression of genes related to regulation of neuron differentiation and expression. It should be noted that the high expression of genes related to muscle filament sliding and actin-myosin filament sliding was observed only in keloids.

When comparing scars that have undergone such a wound healing process with healthy normal skin tissue, wound healing-related genes were discovered preferentially as DEGs rather than genes unique to each scar. Indeed, our present study revealed that scar-free normal skin is an inappropriate control group for determining a unique gene-set for any type of scar. Therefore, we compared keloids, as an irreversible scar, with reversible scars that had undergone the same wound healing process as keloids.

Of the keloid-specific genes discovered by comparison with reversible scars, the Golgin A6 family and *ERICH6B* were prominent in terms of both fold-change and p-value. The Golgin A6 family is a type of coiled-coil protein located in the Golgi apparatus, called golgin [30]. Although the function of the Golgin A6 family is not known, the major functions of related golgins have been determined. Golgin protein maintains the Golgi architecture, is responsible for vesicular traffic, and plays a role in intracellular signal modulation. Since one of the distinguishing characteristics of keloids is the formation of collagen bundles through hypersecretion of collagen, the golgin family which is involved in the intracellular transport of collagen, is highly likely to be a keloid-specific marker. These results are supported other studies comparing keloids and scar-free normal skin (Supplementary Figures 1 and 2). Although little is known about *ERICH6B*, it is highly expressed in hypersecretory fibroblasts found in various lesions of the skin [34]. This result also is supported by other studies that have discovered keloid-specific genes.

To further dissect the pathogenesis of keloids, we conducted ORA to identify keloid specifically activated or inactivated pathways. By comparing keloids with reversible scars, we discovered that 'visual/sensory perception' and 'response to corticosteroids' were highly specific and upregulated pathways for keloids. Interestingly, common symptoms of keloids are itching and pain, both of which are associated directly or indirectly with 'visual/sensory perception.' In addition, corticosteroid injections or ointments have been determined to be effective treatments for keloids, which is highly consistent with our findings [35].

Another finding of our present study is that genes related to 'activation of immune response,' 'antigen processing and presentation of peptide antigen,' 'B cell mediated immunity,' and the 'regulation of T cell activation' were downregulated specifically in keloids. In line with these findings, several studies have underscored the role of the immune cell population in keloids. Jaclyn, et al. reported that CD20+ and CD19+ B cells were significantly increased in keloid tissue compared to normal skin [36]. Murao, et al reported that coculture of keloid fibroblasts with T cell populations enhanced collagen synthesis within fibroblasts [37]. Chen, et al, reported that Treg-associated gene expression was significantly higher in keloids compared to normal skin, which is in agreement with our results [38]. These findings suggest a connection between immune cells and keloids. However, further research is required to validate this suggestion.

Although hypertrophic scars are milder than keloids, they are frequently accompanied by a number of esthetics, functional, and social impairments that can lead to decreased quality of life [39]. Therefore, it is valuable to discover hypertrophic scar-specific gene sets to help in understanding the etiology of hypertrophic scars. As illustrated in Figure 4, a total of 241 HS-specific genes was discovered and is involved in lipid metabolism and water homeostasis. Interestingly, the significance of lipid metabolism in scar formation and wound healing was highlighted in several studies by Louw [40-43]. Proper epidermal hydration is essential for homeostasis of the skin based on the differentiation of epidermal keratinocytes and dermal fibroblasts and modulation of the inflammatory phase [44,45]. Interestingly, in dermatologic treatment, hydration is a recommended method for patients with hypertrophic scars [46].

Conclusions

In this study, using more accurate controls of hypertrophic and normotrophic scars, we discovered keloid-specific pathways and genes. The results of our present study strongly suggest that immune cell immunity and sensory perception are involved in the pathogenesis of keloids. Furthermore, our present study contributed to the understanding of keloid pathogenesis by providing potential biomarkers of keloids such as the golgin A6 family and *ERICH6B*. Extracellular matrix-related processes were also highlighted in both hypertrophic scars and keloids. Finally, we highlight potential keloid-specific biomarkers and expression changes that could be used in future keloids therapeutics.

Acknowledgements

This work was supported by the National Research Foundation of Korea (NRF) grant funded by the Korea government (MSIT) (grant number: 2019R1A2C2003900, 2016R1A5A2945889). This research was also supported by the Bio & Medical Technology Development Program of the National Research Foundation of Korea (NRF) funded by the Ministry of Science & ICT(grant number : 2020M3E5E2040308).

Author Information

All authors helped conceive and design the study and develop the hypothesis. Y.O. and E.L. conducted the laboratory experiment. J.L. conducted the data analysis. J.L, K.M. and M.C. analyzed and interpreted the data and wrote the manuscript. J.H.L and S.H.K. designed experiments, supervised the study.

Data Availability

RNA-seq data that support the findings of this study have been deposited in the GEO under accession number GSE188952. All other relevant data supporting the main findings of this study are available from the corresponding authors upon reasonable request.

Competing Interests

The authors declare no competing interests.

Author's Contribution

Yoojeong Oh and Jaemyun Lyu contributed to this paper equally.

References

1. Jiang D, Rinkevich Y (2020) Scars or regeneration?-Dermal fibroblasts as drivers of diverse skin wound responses. Int J Mol Sci 21:617.
2. Wang Z, Zhao W, Cao Y, Liu Y, Sun Q et al. (2020) The roles of inflammation in keloid and hypertrophic scars. Front Immunol 11:603187.
3. Li K, Nicoli F, Cui C, Xi W, Al-Mousawi A, et al. (2020) Treatment of hypertrophic scars and keloids using an intralesional 1470 nm bare-fibre diode laser: A novel efficient minimally-invasive technique. Sci Re 10:21694.
4. Ogawa R (2017). Keloid and hypertrophic scars are the result of chronic inflammation in the reticular dermis. Int J Mol Sci 18:606.
5. Eto H, Suga H, Aoi N, Kato H, Doi K, et al. (2012) Therapeutic potential of fibroblast growth factor-2 for hypertrophic scars: upregulation of MMP-1 and HGF expression. Lab Invest 92:214-223.
6. Trace A, Enos C, Mantel A, Harvey V (2016) Keloids and hypertrophic scars: A spectrum of clinical challenges. Am J clin Dermatol 17:201-223.
7. Gauglitz G, Korting H, Pavicic T, Ruzicka T, Jeschke M (2011) Hypertrophic scarring and keloids: Pathomechanisms and current and emerging treatment strategies. Mol Med 17:113-125.
8. Huang C, Murphy G, Akaishi S, Ogawa R (2013) Keloids and hypertrophic scars: Update and future directions. Plast Reconstr Surg Glob Open 1:e25.
9. Atiyeh B, Costagliola M, Hayek S (2005) Keloid or hypertrophic scar: The controversy: Review of the literature. Ann Plast Surg 54:676-680.
10. Swann D, Garg H, Jung W, Hermann H (1985) Studies on human scar tissue proteoglycans. J Invest Dermatol 84:527-531.
11. Limandjaja G, Niessen F, Scheper R, Gibbs S (2021) Hypertrophic scars and keloids: Overview of the evidence and practical guide for differentiating between these abnormal scars. Exp Dermatol 30:146-161.
12. Carswell L, Borger J (2021) Hypertrophic scarring keloids. StatPearls.
13. Onoufriadis A, Hsu C, Ainali C, Ung C, Rashidghamat E, et al. (2018) Time series integrative analysis of RNA sequencing and MicroRNA expression data reveals key biologic wound healing pathways in keloid-prone individuals. J Invest Dermatol 138:2690-2693.
14. Wu J, Duca E, Espino M, Gontzes A, Cueto I, et al. (2020) RNA sequencing keloid transcriptome associates keloids with Th2, Th1, Th17/Th22, and JAK3-skewing. Front Immunol 11:597741.

15. Hahn J, Glaser K, McFarland K, Aronow B, Boyce S, et al. (2013) Keloid-derived keratinocytes exhibit an abnormal gene expression profile consistent with a distinct causal role in keloid pathology. Wound Repair Regen 21:530-544.

16. Hsu C, Lin H, Harn H, Ugawa R, Wang Y, et al. (2018) Caveolin-1 controls hyperresponsivenessto mechanical stimuli and fibrogenesis-associated RUNX2Activation in keloid fibroblasts. J Invest Dermatol 138:208-218.

17. Matsumoto N, Aoki M, Okubo Y, Kuwahara K, Eura S, et al. (2020) Gene expression profile of isolated dermal vascular endothelial cells in keloids. Front Cell Dev Biol 8:658.

18. Martin M (2011) Cutadapt removes adapter sequences from high-throughput sequencing reads. EMBnet J 17(1), 10

19. Dobin A, Davis C, Schlesinger F, Drenkow J, Zaleski C, et al. (2013) STAR: Ultrafast universal RNA-seq aligner. Bioinformatics 29:15-21.

20. Anders S, Pyl P, Huber W (2015) HTSeq-a python framework to work with high-throughput sequencing data. Bioinformatics 3:166-169.

21. Krijthe J (2016) Rtsne: T-distributed stochastic neighbor embedding using a barnes-hut implementation.

22. Ritchie M, Phipson B, Wu D, Hu Y, Law, et al. (2015) Limma powers differential expression analyses for RNA-sequencing and microarray studies. Nucleic Acids Res 43:e47

23. Robinson M, McCarthy D, Smyth G (2009) edgeR: A bioconductor package for differential expression analysis of digital gene expression data. Bioinformatics 26:139-140.

24. Love M, Huber W, Anders S (2014) Moderated estimation of fold change and dispersion for RNA-seq data with DESeq2. Genome Biol 15:1-21.

25. Kuleshov M, Jones M, Rouillard A, Fernandez N, Duan Q, et al. (2016) Enrichr: A comprehensive gene set enrichment analysis web server 2016 update. Nucleic acids research. 44:W90-97.

26. Gontarz P, Fu S, Xing X, Liu S, Miao B, et al. (2020) Comparison of differential accessibility analysis strategies for ATAC-seq data. Sci Rep 10:10150.

27. Tuan TL, Nichter L (1998) The molecular basis of keloid and hypertrophic scar formation. Mol Med Today. 4:19-24.

28. Tanaka A, Hatoko M, Tada H, Iioka H, Niitsuma K, et al. (2004) Expression of p53 family in scars. J Dermatol Sci 34:17-24.

29. Amadeu T, Braune A, Mandarim-de-Lacerda C, Porto L, Desmoulière A, et al. (2003) Vascularization pattern in hypertrophic scars and keloids: A stereological analysis. Pathol Res Pract 199:469-473.

30. Ehrlich H, Desmoulière A, Diegelmann R, Cohen I, Compton C, et al. (1994) Morphological and immunochemical differences between keloid and hypertrophic scar. Am J Pathol 145:105-113.

31. Witkos T, Low M (2016) The golgin family of coiled-coil tethering proteins. Front Cell Dev Biol 3:86.

32. Stadelmann W, Digenis A, Tobin G (1998) Physiology and healing dynamics of chronic cutaneous wounds. Am J Surg 176:26S-38S.

33. Midwood K, Williams L, Schwarzbauer J (2004) Tissue repair and the dynamics of the extracellular matrix. Int J Biochem Cell Biol 36:1031-1037.

34. Theoret C (2005) The pathophysiology of wound repair. Vet Clin N Am Equine Pract. 21:1-13.

35. The Human Protein Atlas. ERICH6B.

36. Ogawa R, Akaishi S, Kuribayashi S, Miyashita T (2016) Keloids and hypertrophic scars can now be cured completely: recent progress in our understanding of the pathogenesis of keloids and hypertrophic scars and the most promising current therapeutic strategy. J Nippon Med SCH 83:46-53.

37. Jaclyn B, Hararnt A, Navarro-Alvarez N, Wang Z, Bokhoven A, et al. (2020) Characterization of immune cells found in keloid versus normal skin tissue. J Immunol 14:23.

38. Murao N, Seino K, Hayashi T, Ikeda M, Funayama E, et al. (2014) Treg-enriched CD4+ T cells attenuate collagen synthesis in keloid fibroblasts. Exp Dermatol 23:266-271.

39. Chen Y, Jin Q, Fu X, Qiao J, Niu F (2019) Connection between T regulatory cell enrichment and collagen deposition in keloid. Exp Cell Res. 383:111549.

40. Bock O, Schmid-Ott G, Malewski P, Mrowietz U (2006) Quality of life of patients with keloid and hypertrophic scarring. Arch Dermatol Res. 297:433-438.

41. Louw L, Engelbrecht A, Cloete F, van der Westhuizen J, Dumas L (1997) Impairment in the fatty acid composition of keloids. Adv Exp Med Biol 400B:905-910.

42. Louw L (2000) Keloids in rural black South Africans. Part 1: General overview and essential fatty acid hypotheses for keloid formation and prevention. Prostaglandins Leukot Essent Fatty Acids 63:237-245.

43. Louw L, Dannhauser A (2000) Keloids in rural black South Africans. Part 2: Dietary fatty acid intake and total phospholipid fatty acid profile in the Page 5 of 6 blood of keloid patients. Prostaglandins Leukot Essent Fatty Acids 63:247-253.

44. Louw L (2000) Keloids in rural black South Africans. Part 3: A lipid model for the prevention and treatment of keloid formations. Prostaglandins Leukot Essent Fatty Acids 63:255-262.

45. Wang R, Mao Y, Zhang Z, Li Z, Chen J, et al. (2016) Role of verapamil in preventing and treating hypertrophic scars and keloids. Int Wound J 13:461-468.

46. Puri N, Talwar A (2009) The efficacy of silicone gel for the treatment of hypertrophic scars and keloids. J Cutan Aesthet Surg 2:104-106.